

## First-principles simulations of liquid ZnTe

Manish Jain, Vitaliy V. Godlevsky, Jeffrey J. Derby, and James R. Chelikowsky  
*Department of Chemical Engineering and Materials Science, Minnesota Supercomputing Institute,  
 University of Minnesota, Minneapolis, Minnesota 55455*

(Received 3 May 2001; revised manuscript received 3 October 2001; published 27 December 2001)

We report the results of *ab initio* molecular-dynamic simulations of liquid ZnTe near the melting point temperature. In agreement with experiment, we find that *l*-ZnTe retains its open tetrahedral environment upon melting with a coordination near four. In addition, we find atoms of Te in *l*-ZnTe often form transitory chains just as in *l*-CdTe. We compare our calculated structure factor to experiment and also determine the conductivity of the melt. *l*-ZnTe has a semiconductorlike conductivity similar to CdTe. We also calculate the dynamic properties of the liquid and predict self-diffusion constants of  $D_{\text{Zn}}=1.0\times 10^{-4}$  cm<sup>2</sup>/s and  $D_{\text{Te}}=3.2\times 10^{-5}$  cm<sup>2</sup>/s.

DOI: 10.1103/PhysRevB.65.035212

PACS number(s): 72.80.Ph, 31.15.Ar, 71.15.Pd

### I. INTRODUCTION

Over the past few years, *ab initio* molecular dynamics has become a popular tool for the investigation of materials. Liquids and amorphous semiconductors are examples of disordered materials to which this technique has been applied extensively. For example, group IV elements—Si and Ge have been studied in their amorphous and liquid states.<sup>1–5</sup> Also, several III-V compounds such as GaAs, GaSb, and InP (Refs. 6–9) have been studied using this technique. However, despite their technological importance, there have been very few studies of II-IV semiconductor liquids. Except for a recent theoretical study of CdTe (Ref. 10), *ab initio* molecular dynamics has not been applied to this class of semiconductors. Similarly, there have been very few experiments for examining the structure of II-VI liquids.<sup>11–13</sup>

Among II-VI semiconductors, ZnTe and CdTe, are materials of special technological interest. ZnTe is used as a substrate for the growth of CdTe. Heterostructures based on ZnTe and HgTe are used for infrared optics. When doped with vanadium, ZnTe becomes a photorefractive semiconducting material. This has potential applications for optical power limiting. Also ZnTe has been investigated for its uses as visible light-emitting semiconductor laser.<sup>14</sup> Besides these technological applications, liquid ZnTe (*l*-ZnTe) is also a material of fundamental interest. *l*-ZnTe (like *l*-CdTe) exhibits properties that are different from liquid III-V and group IV liquids. According to an empirical rule by Joffe and Regel,<sup>15</sup> a melt retains semiconducting properties (despite losing its long-range order) only if short-range order of the crystalline phase is preserved. *l*-ZnTe is believed to retain an open tetrahedral structure with coordination number of four.<sup>12,13</sup> Although dc electrical conductivity jumps upon melting, the conductivity of the melt increases with temperature, i.e., *l*-ZnTe is a semiconductor.<sup>16</sup> This is in contrast with III-V and group IV melts, which become more closed packed upon melting. The coordination numbers of these semiconductors increase to  $\sim 6$  (Refs. 4–7). They undergo a semiconductor to metal transition upon melting as the conductivity of the liquid decreases upon further increases in temperature.<sup>16</sup>

Another significant difference between *l*-ZnTe (and

*l*-CdTe) and III-V compounds is in the degree of dissociation. Using thermodynamic<sup>18</sup> estimates, the curvature of the liquidus can be related to the degree of dissociation of cations and anions and to the entropy change in the solid-liquid transition. According to the phase diagram of ZnTe,<sup>16</sup> at the congruent point, the liquidus has a sharp hyperbolic curvature.<sup>17</sup> This implies the conservation of heterogeneous bonds. The cations prefer to be in a local environment of anions and vice versa. This is in contrast to III-V compounds, where the local environment is significantly changed. In III-V liquids a significant percentage of heteropolar bonds are destroyed and a large number of stoichiometric defects such as homopolar bonds are introduced.<sup>19,20</sup>

In order to investigate the structural, electronic, and dynamical properties of *l*-ZnTe near its melting temperature, we perform *ab initio* molecular-dynamics study. We focus our studies by comparing ZnTe to previous studies on CdTe.

### II. COMPUTATIONAL METHODS

These calculations were performed using the pseudopotential density-functional method (PDFM) using a plane-wave basis set.<sup>4,10,19</sup> The PDFM eliminates the core electrons from consideration and focuses only on the chemically active valence electrons. This procedure has a number of advantages over “all-electron” potentials. Since only the eigenstates of the valence electrons are required, the number of eigenvalue pairs is significantly reduced, especially for heavier elements. Moreover, the length scale of the basis is set by the valence electrons. The nodal structure of the core states is removed and the resulting pseudopotential does not contain any singularities. This permits one to use simple basis such as plane waves and obtain a highly converged solution with relatively few plane waves.

Usually the distinction between core and valence states is clear; however, in the case of II B elements such as Zn, Cd or Hg, it is not obvious whether the filled *d* orbitals should be considered a part of the core or treated explicitly as valence electrons. Since these orbitals overlap significantly with *s* orbitals, they can exhibit some chemical activity. On the other hand, there are a couple of disadvantages in treating them explicitly. First, it would increase the number of elec-

TABLE I. Lattice constants and bulk moduli for zinc-blende phase of ZnTe calculated with different Zn potentials. The cutoff radii used to generate Zn potentials are presented.

	$a$ (Å)	$B$ (GPa)	$r_c$ (for $s/p/d$ in Å)
Zn <sup>2+</sup> 4s <sup>2</sup> 4p <sup>0</sup> 4d <sup>0</sup>	5.69	59	1.38/1.38/1.90
Zn <sup>2+</sup> 4s <sup>2</sup> 4p <sup>0</sup> 4d <sup>0</sup>			
Partial-core correction	5.95	49	1.38/1.38/1.90
Zn <sup>12+</sup> 3d <sup>10</sup> 4s <sup>2</sup> 4p <sup>0</sup>	6.07	54	1.38/1.27/1.69
Experiment	6.10	51 (Refs. 25,26)	

trons per cation-anion pair from 8 to 18. This increases the number of eigenvalues that are needed to be calculated. Second, since the potential when the  $d$  orbitals are occupied is much more stronger than when they are unoccupied, more plane waves are required for an equivalently converged solution.

We address this problem using the “partial-core correction.”<sup>21</sup> In the partial-core treatment, the  $d$  electrons are included implicitly in obtaining a valence-core exchange potential, but the wave functions for the  $d$  orbitals are fixed by atomic calculations. This method has been successfully used in the case of CdTe (Ref. 10).

In our calculations, we have done extensive testing on this issue. We constructed three Zn pseudopotentials: one with  $3d$  treated as core, another with  $3d$  treated within the partial-core correction and third with  $3d$  treated explicitly as valence electrons. These *ab initio* pseudopotentials were generated in the Troullier-Martins<sup>22</sup> form with Ceperley-Alder<sup>23</sup> form for correlation. The nonlocal part of the pseudopotentials was taken to be in the Kleinman-Bylander<sup>24</sup> form. We examined the crystalline properties of ZnTe using a two-atom primitive cell for all these pseudopotentials. We used ten irreducible  $k$  points in the Brillouin zone and a cutoff of 40 Ry. Table I shows the crystalline structural parameters (lattice constant and bulk modulus) of ZnTe for all three pseudopotentials. As is evident, partial-core correction substantially improves upon the pseudopotential without a partial-core correction and brings the lattice constant within  $\sim 2\%$  and bulk modulus within  $\sim 5\%$  of experiment. Further, Fig. 1 shows the band structure of ZnTe calculated with  $3d$  treated explicitly and using partial-core correction. Around the Fermi level, both band structures have an excellent agreement. When treated explicitly the  $3d$  levels do push the Te  $s$  levels down by  $\sim 0.5$  eV, but since these are about 10 eV below the Fermi level they do not effect any electronic properties.

In addition to examining the Zn-Te interactions within the crystalline environment, we performed an additional test on the Zn pseudopotentials. We examined the behavior of Zn in liquid ZnTe using the pseudopotential with the  $3d$  states treated explicitly and the pseudopotential with a partial-core correction. We examined the dynamical behavior of the liquid by considering a small unit cell. We took a conventional zinc-blende cell (eight atoms) and examined the Zn self-diffusion constant over a 1.5 ps simulation. We found the two potentials yielded the same self-diffusion constant to within

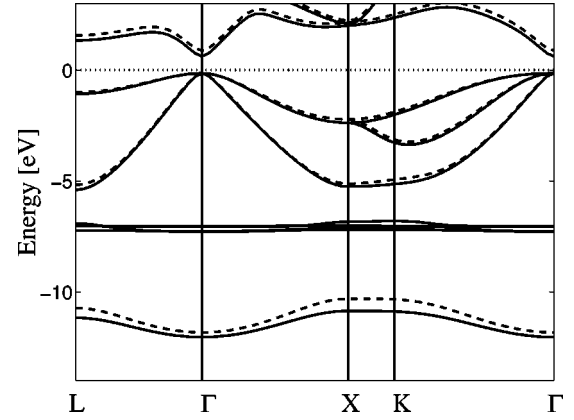


FIG. 1. Band structure of zinc-blende ZnTe. The solid lines show results where  $3d$  electrons are treated as valence electrons. The dashed lines show results where  $3d$  electrons are treated via the partial-core correction (see text).

$\sim 5\%$ . Finally, we examined the radial distribution function for this small system and found no significant changes between the two pseudopotentials. In short, we are confident that our simulations with the partial-core pseudopotential do a reasonable job of replicating the liquid-state properties of ZnTe.

In order to model the liquid, we considered a supercell with periodic boundary conditions. 64 atoms (32 Zn and 32 Te) were placed inside this supercell. The size of this cubic supercell was  $2a$ , where  $a$  is lattice parameter for a conventional fcc unit cell. Most “*ab initio*” simulations of the liquid state do not attempt to find the equilibrium density. Instead the simulations are usually fixed at the experimental density. Here  $a$  was chosen such that the density matched the experimental density of the liquid,  $4.97$  g/cm<sup>3</sup> (Ref. 12). Studies using interatomic potentials have shown that 64-atom system is large enough to capture the essential features.<sup>27</sup>

In examining the liquid state, a difficult issue is preparing the liquid-state ensemble. One can only use time-averaged statistical average to characterize the liquid, unlike solids where the positions are fixed. We employed Langevin dynamics to prepare the liquid-state ensemble.<sup>28,29</sup> The trajectory of each atom was computed using the Langevin equation of motion

$$m_i \frac{d\mathbf{v}_i}{dt} = -\gamma m_i \mathbf{v}_i + \mathbf{R}_i(\gamma, T) + \mathbf{F}_i, \quad (1)$$

where  $\mathbf{F}_i$  is the force on the  $i$ th atom,  $m_i$  the mass of the atom, and  $\gamma$  the viscosity of the fictive heat bath. The atoms are subjected to rapidly varying random forces  $\mathbf{R}_i(\gamma, T)$ . These random forces, functions of both temperature and viscosity, are described by the fluctuation-dissipation theorem. The random forces and viscosity couple the system to a hypothetical heat bath. The time step for integration was 250 a.u. The interatomic forces  $\mathbf{F}_i$  were calculated quantum mechanically from *ab initio* pseudopotential wave functions on a plane-wave basis set<sup>29</sup> using the Hellmann-Feynman theorem. With respect to some technical issues, the charge den-

sity required to construct a self-consistent field was calculated at the  $\Gamma$  point in the supercell. The energy cutoff for the wave functions was 9 Ry.

In order to test the applicability of this cutoff of 9 Ry we calculated the lattice constant of crystalline ZnTe. It agreed to within 0.2% of the value calculated using 40 Ry. We also compared the band structure calculated using 9 and 40 Ry. The root-mean-square error in the eigenvalues was  $\sim 0.05$  eV. Further, we did a small molecular-dynamics simulation of liquid ZnTe as before. Again the diffusion constants agreed to within  $\sim 5\%$  with the 40 Ry simulation.

The *l*-ZnTe ensemble was created by randomly placing the atoms in the supercell with the constraint that no two atoms be closer than 90% of the bond length in the crystal. Starting from a random configuration (as compared to crystalline configuration) has the advantage that significant energy is imparted to the system since the configuration is far from the ground state. The dissipation of this energy allows activation of compositional defects. Also, a random configuration introduces stoichiometric defects that may be inaccessible to the system. The ensemble was initially thermalized at a fictive temperature of 6000 K for about 2.5 ps. In this time, the average diffusion distance of an atom becomes comparable to the size of the conventional unit cell. This ensures one that a proper mixing of atoms occurs and that any bias of the system to initial conditions is suppressed. The system was then cooled to 1318 K (250 K below the melting temperature) in 4.5 ps. Density functionals usually underestimate the melting temperature.<sup>30</sup> Since we want to simulate the liquid near its melting temperature, we chose a temperature near the expected theoretical melting temperature. It is important to create the liquid ensemble by cooling from above the melting point. Otherwise, the system would never melt given the time scale, and the hysteresis involved in homogeneous melting. The liquid was then thermalized at 1318 K for 6.5 ps. Statistics were collected over the final 4 ps of the simulation, where the viscosity was turned off. When the viscosity is set to zero, the random forces are also set to zero via the fluctuation-dissipation theorem. The dynamics of our ensemble become “true” dynamics as the ensemble is transformed from a canonical to microcanonical one.

### III. PROPERTIES OF LIQUID ZINC TELLURIDE

#### A. Structural properties

One strength of “quantum” molecular dynamics is that both the electronic and nuclear degrees of freedom can be simultaneously examined. Figure 2 shows a typical snapshot of the liquid at one of the time steps during the last 6.5 ps. The isosurface of the electronic charge density taken at half its maximum value (in the supercell) is shown along with the nuclear positions. It is clear from this figure that the liquid is ionic in nature. We examine the character of the wave functions and find that the charge near the Te atoms have *p* electron character while the wave functions localized on the Zn cations are *s*-like. This is not surprising and is consistent with the chemistry of the crystalline state.

A key measure of the liquid-state structure is the pair-correlation function or the radial-distribution function  $g(r)$ .

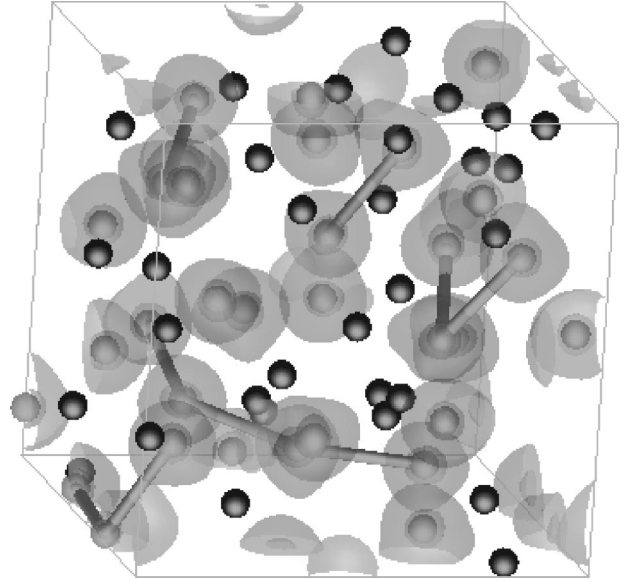


FIG. 2. A snapshot showing a typical *l*-ZnTe structure in the supercell (see text). Atoms of Zn are represented by dark spheres, atoms of Te are shown by light spheres.

Using the atomic positions for each time step, and averaging the positions over the last 4 ps of the simulation, we obtain  $g(r)$  as shown in Fig. 3. The first peak is at  $R_{\max 1} = 2.64 \text{ \AA}$ , second peak is at  $R_{\max 2} = 4.38 \text{ \AA}$ , and the first minimum corresponding to a complete shell is at  $R_{\min} = 3.35 \text{ \AA}$ . In the crystalline phase the first and the second nearest neighbors are at 2.64 and 4.32  $\text{\AA}$  respectively, which agrees very well with the positions of the peaks in  $g(r)$ . From Fig. 3, it is clear that the liquid lacks any long-range correlations. The pair correlation attenuates strongly after the first peak, i.e., the atoms do not correlate with their images in neighboring periodically replicated cells. This confirms, *a posteriori*, that a 64-atom system is large enough for the simulation. Figure 3 also shows the experimentally obtained  $g(r)$ . The theoretical curve is in good agreement with the experimental one.

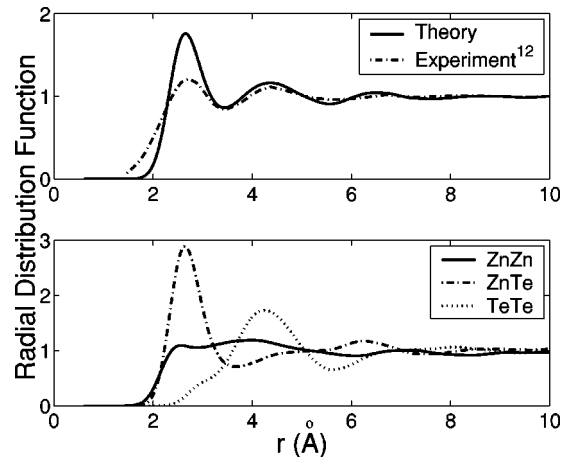


FIG. 3. Total pair-correlation function [both theory and experiment (Ref. 12)] in the top panel and partial pair-correlation functions in the bottom panel.

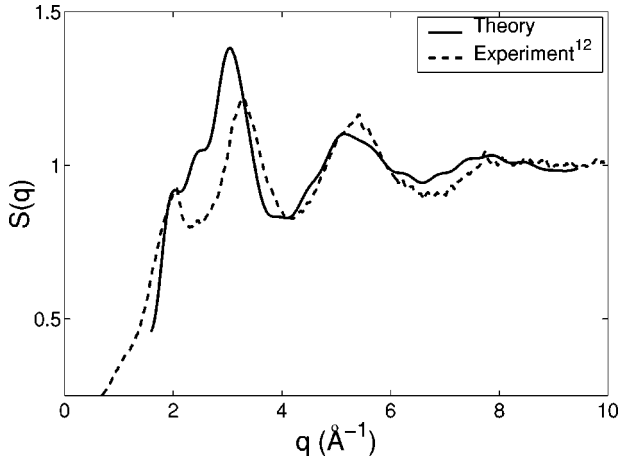


FIG. 4. Total structure factors. For *l*-ZnTe at the melting temperature, we compare our data with available experiment (Ref. 12) (dashed line).

Figure 3 also shows the partial radial-distribution functions. These are calculated by averaging over the positions of atoms of each type for the last 4 ps of the simulation. The peak at  $R_{\max 1} = 2.64 \text{ \AA}$  in the total pair-correlation function comes from the corresponding peak in  $g_{\text{Zn-Te}}(r)$  while the second peak (at  $R_{\max 2} = 4.38 \text{ \AA}$ ) is mainly from  $g_{\text{Te-Te}}(r)$ . Also,  $g_{\text{Zn-Zn}}(r)$  indicates that the Zn atoms are randomly distributed (with the constraint that no two atoms can be closer than  $R = 2.1 \text{ \AA}$ ).

To compare our calculations with neutron-scattering experiments,<sup>12</sup> we calculate the total structure factor function, as a linear combination of the partial structure factors  $S_{\text{Zn-Zn}}(q)$ ,  $S_{\text{Zn-Te}}(q)$ , and  $S_{\text{Te-Te}}(q)$ , normalized by scattering lengths  $\alpha_{\text{Zn}}$  and  $\alpha_{\text{Te}}$ :

$$S(q) = \frac{\alpha_{\text{Zn}}^2 S_{\alpha\alpha}(q) + 2\alpha_{\text{Zn}}\alpha_{\text{Te}} S_{\alpha\beta}(q) + \alpha_{\text{Te}}^2 S_{\beta\beta}(q)}{\alpha_{\text{Zn}}^2 + \alpha_{\text{Te}}^2}. \quad (2)$$

The ratio of the scattering lengths is taken to be  $\alpha_{\text{Zn}}/\alpha_{\text{Te}} = 5.68/5.8$  (Ref. 31). Partial structure factors are obtained from partial radial-distribution functions by a fourier transformation:

$$S_{\alpha\beta}(q) = \delta_{\alpha\beta} + 4\pi\rho_{\alpha\beta} \int_0^{\infty} [g_{\alpha\beta} - 1] \frac{\sin(2\pi qr)}{2\pi qr} r^2 dr, \quad (3)$$

where  $\rho_{\alpha\beta}$  is partial density.

Figure 4 shows the total structure factor as obtained from our simulation and from experiment. The first peak position matches very well, but for the second peak position there is a discrepancy of 6%. Despite this difference, the overall agreement between these structure factors is good. Upon varying the density, we find that the structure factor does not change significantly. The overall shape remains similar and the peaks still align well with experiment. This is consistent with our earlier calculations on III-V semiconductors that have shown that  $\pm 10\%$  variations in volume do not affect the structure of the liquid. Metallic liquids<sup>32</sup> also show similar insensitivity to density.

TABLE II. Total and partial coordination numbers for ZnTe and CdTe at their melting temperatures.

	$C_{\text{tot}}$	$C_{\alpha\text{Te}}$	$C_{\alpha\alpha}$	$C_{\text{Te-Te}}$	CDN
$\alpha = \text{Zn}$	4.6	3.4	2.0	0.6	0.4
$\alpha = \text{Cd}$	4.4	3.3	1.5	0.9	0.4

We estimate the total and partial coordination numbers from their corresponding pair-correlation function as  $C_{\alpha\beta} = \int_0^{R_{\min}} 4\pi r^2 g_{\alpha\beta}(r) dr$ , where  $R_{\min}$  is the first minimum in the total radial-distribution function. As a measure of the concentration of stoichiometric defects in the system, we introduce a composition disorder number (CDN). It is defined as a ratio of homogeneous and heterogeneous bonds,  $\text{CDN} = (C_{\text{Zn-Zn}} + C_{\text{Te-Te}})/2C_{\text{Zn-Te}}$ . For zinc-blende structure CDN is zero while for a perfectly disordered crystal CDN is one. Table II shows the partial coordination numbers and CDN of *l*-ZnTe. The average number of neighbors in the first shell is 4.6. This indicates that *l*-ZnTe retains its open structure upon melting, unlike group IV and III-V liquids that become closed packed. This is also in agreement with the assumption that the degree of dissociation of heterogeneous bonds in *l*-ZnTe is smaller than III-V liquids. Table II also shows the coordination numbers for *l*-CdTe (Ref. 10) near its melting temperature. The similarity between the two liquids is evident.

We also calculate the angular distribution function, or pair-correlation function of order higher than two. Figure 5 shows the total angular distribution function  $g(\theta)$ , which is calculated as an average of angle defined between the reference atom, the nearest atom, and a vector drawn to all atoms within a radius  $R_{\min}$  of the reference atom. The distributions are normalized by  $\sin(\theta)$  because a homogeneous distribution of atoms would correspond to  $\sin(\theta)$ . From Fig. 5, it is clear that the predominant angles correspond to  $\sim 60^\circ$ ,  $\sim 100^\circ$ , and  $\sim 150^\circ$ . One may interpret the first two angles as corresponding to the closed-packed angle and tetrahedral angles. The

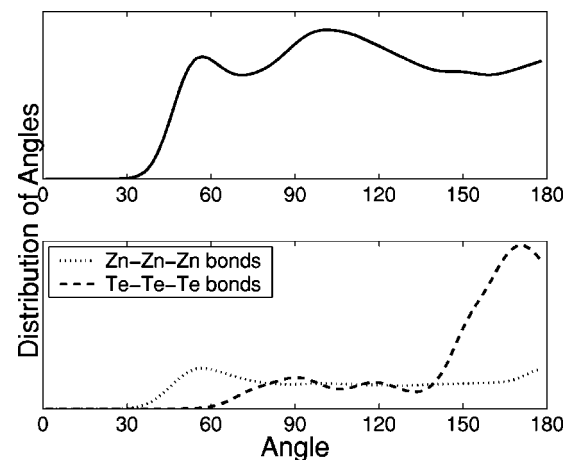


FIG. 5. Total angular distribution (in arbitrary units) of bond angles in the top panel. Angular distribution of bond angles in Te and Zn clusters in the bottom panels. The distributions are normalized by  $\sin(\theta)$ .

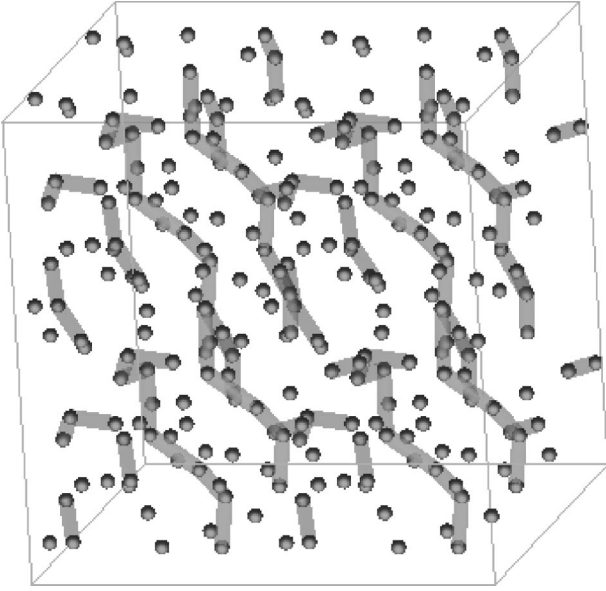


FIG. 6. Structure of Te chains in  $l$ -ZnTe. The box corresponds to  $2 \times 2 \times 2$  supercell geometry. Only atoms of Te and bonds between them are shown.

peak  $\sim 150^\circ$  comes from Te-Te-Te angle distribution (which is also shown in Fig. 5). This angle is reminiscent of helical Te chains in elemental  $l$ -Te (Refs. 33,34). Indeed, snapshots of the  $l$ -ZnTe show such chains in which  $\sim 40\%$  of Te atoms participate. This is very similar to the Te chains in  $l$ -CdTe (Ref. 10). Figure 6 shows the atomic configuration in a typical snapshot of  $l$ -ZnTe. Only the Te atoms are shown for clarity. Atoms are considered bonded if the distance between them is less than  $R_{\min}$ . The figure shows that Te atoms do indeed form chains. This is in contrast with Zn-Zn-Zn bond-angle distribution shown in Fig. 5. The predominant angle is  $\sim 60^\circ$ , i.e., atoms of Zn form closed-packed clusters.

### B. Electronic properties

The optical conductivity of a system can be calculated from a knowledge of the electronic structure. According to the Kubo-Greenwood<sup>35</sup> expression the real part of conductivity can be calculated as

$$\sigma_r(\omega) = \frac{2\pi e^2}{3m^2\omega\Omega} \sum_{n,m} \sum_{\alpha=x,y,z} |\langle \psi_m | p_\alpha | \psi_n \rangle|^2 \times \delta(E_n - E_m - \hbar\omega), \quad (4)$$

where  $E_i$  and  $\psi_i$  are eigenvalues and eigenfunctions, and  $\Omega$  is the volume of the supercell. Dipole transition elements were sampled at the  $\Gamma$  point in the Brillouin zone. The lowest 300 eigenstates were included in the summation. The real part of the optical conductivity is shown in Fig. 7. We included five configurations chosen at random from the last 4 ps of the simulation. This appears to be sufficient for a reasonable convergence of the conductivity. The electron temperature (in the Fermi-Dirac function) was taken to be zero in all these calculations. From Fig. 7, it is clear that  $l$ -ZnTe has a semiconductor-type conductivity: real part of the con-

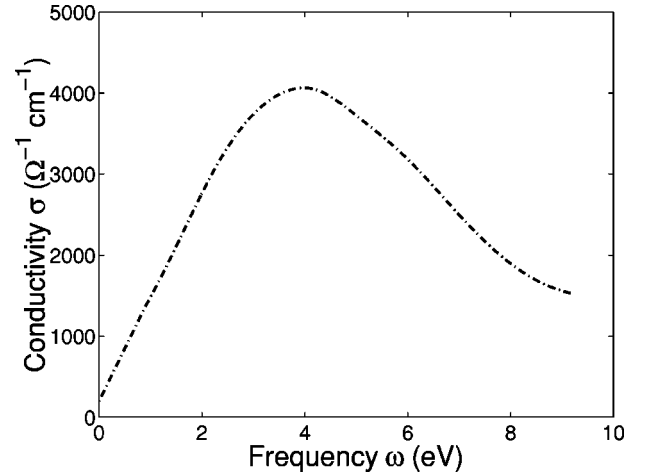


FIG. 7. Real part of optical conductivity.

ductivity does not have a metallic Drude-like dependence [ $\sigma(\omega) \sim \sigma_0 / (1 + \omega^2\tau^2)$ ] as liquid IV and III-V semiconductors have. The frequency-dependent conductivity peaks  $\sim 4$  eV and then asymptotically goes to zero as  $1/\omega^2$ . The dc conductivity value ( $\omega=0$ ) is obtained by linearly extrapolating from  $\omega \rightarrow 0$ . We obtain a value of  $\sim 100 \Omega^{-1} \text{cm}^{-1}$ , which is slightly larger than the experimental value<sup>16</sup> of  $40 \Omega^{-1} \text{cm}^{-1}$ . This overestimate of the conductivity is not surprising given the uncertainties in the theoretical calculations and experimental measurements. For example, the experimental values for the conductivity of liquids often vary by a factor 2–3 (Ref. 10). Further, it is known that the conductivity is a strong function of temperature.<sup>16</sup> At  $\sim 60$  K above the melting temperature, the conductivity rises very rapidly. As discussed earlier, the temperature of our liquid is subjected to some uncertainty and could result in the overestimate of conductivity. To investigate this issue further, we cooled the liquid by another 300 K. There were no differences in the structural properties of the liquid. We chose several configurations from the final 1 ps of the cooled liquid and calculated the conductivity. The conductivity did not change significantly. However, we did find a strong variance with the pressure. If the density of the liquid is increased by  $\sim 10\%$ , the conductivity increases by nearly an order of magnitude. Additionally, our use of the Kohn-Sham eigenvalues in Eq. (4) is suspect since the Kohn-Sham eigenvalues underestimate the band gap.<sup>36</sup> As a consequence, we expect our calculations to yield an enhanced conductivity.

### C. Dynamic properties

By following the atomic positions and velocities of the atoms in the liquid state as a function of time, we can calculate the vibrational density of states and diffusion constants of Zn and Te in  $l$ -ZnTe. To obtain the true dynamics, we set the viscosity parameter to zero and followed the trajectory of each atom in the liquid for 4 ps of the simulation (time window). The diffusion constant is given as

$$D_i = \lim_{t \rightarrow \infty} \frac{\langle [R_i(t) - R_i(0)]^2 \rangle}{6t}, \quad (5)$$

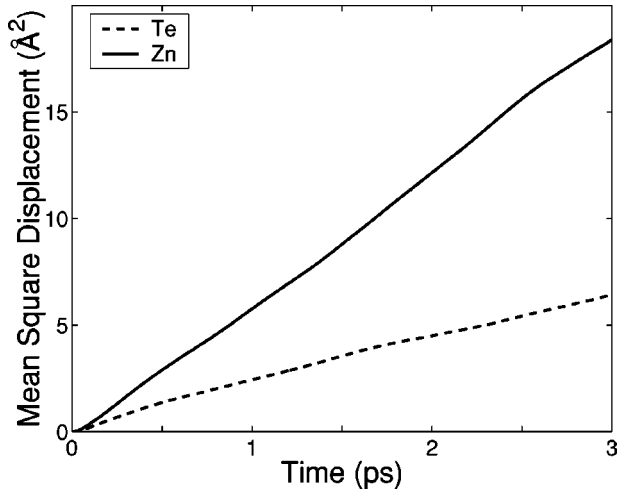


FIG. 8. Mean-square displacement as a function of time.

where  $R_i(t)$  is the position of the  $i$ th atom after time  $t$ . The average is over all atoms of the same type in the unit cell. Figure 8 shows the mean-square displacement as a function of time. The resulting diffusion coefficients are  $D_{\text{Zn}} = 1.0 \times 10^{-4} \text{ cm}^2/\text{sec}$  and  $D_{\text{Te}} = 3.2 \times 10^{-5} \text{ cm}^2/\text{sec}$ .

We also calculate the velocity autocorrelation function  $Z(t)$  defined as

$$Z(t) = \frac{\langle v_i(t)v_i(0) \rangle}{\langle v_i(0)v_i(0) \rangle}, \quad (6)$$

where  $v_i(t)$  is the atomic velocity of the  $i$ th atom after time  $t$ . The average is also over all atoms in the unit cell for the total velocity autocorrelation function  $Z(t)$ , and over all atoms of same type for  $Z_\alpha(t)$  ( $\alpha = \text{Zn, Te}$ ). The diffusion constants can be calculated as

$$D_i = \frac{k_b T}{m_i} \int_0^\infty Z_i(t) dt, \quad (7)$$

where  $m_i$  is the mass of atom of type  $i$ ,  $k_b$  is the Boltzmann constant, and  $T$  is the temperature. The diffusion constants calculated this way match those calculated above to within 10%.

The vibrational density of states that is proportional to the Fourier transform of  $Z(t)$  is shown in Fig. 9. Before Fourier transforming the  $Z(t)$  a Hamming window<sup>37</sup> was applied to it. We checked several different windowing functions that they did not affect the overall shape and peak positions in the curve. As can be seen in the figure, there are several modes at zero frequency. Presence of these modes implies that the atoms move (i.e., the system is liquidlike and is not an amorphous solid). Despite this liquid behavior, there are several

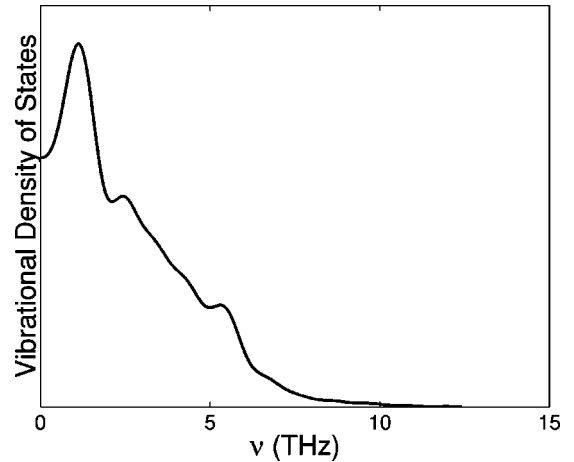


FIG. 9. Vibrational density of states in the liquid.

peaks corresponding to crystalline acoustic ( $\sim 1.5$ – $5$  THz), and optical ( $\sim 5$ – $6$  THz) modes.<sup>25</sup> This reflects the presence of local order within the melt.

#### IV. CONCLUSION

We performed *ab initio* molecular-dynamic simulations of  $l$ -ZnTe near its melting temperature. The calculated structure factor agrees well with experiment.<sup>12</sup> In agreement with experiment, we find that  $l$ -ZnTe retains its open structure in the melt with a coordination number  $\sim 4$ , as for  $l$ -CdTe (Ref. 10). This is very different from group IV and III-V liquids, which have coordination number  $\sim 6$  upon melting.  $l$ -ZnTe also behaves like  $l$ -CdTe in terms of the degree of dissociation in the melt. Unlike group III-V liquids, significant number of heterogeneous bonds are preserved. We also find that atoms of Te form chains in  $l$ -ZnTe as in  $l$ -CdTe. We find that  $l$ -ZnTe also has a semiconductorlike conductivity.

In group IV and III-V semiconductors where the ionicity is smaller, in the liquid state the entropy favors a disordered and closed-packed structure. We believe in  $l$ -ZnTe (as in  $l$ -CdTe) homogeneous bonds are not preferred because the ionicity is higher. This limits the miscibility of different types of atoms (compared to group IV and III-V liquids). Thus, the internal energy opposes the entropy and prevents a closed packed, randomly mixed phase. The higher ionicity also prevents delocalization of electrons and leads to semiconductorlike properties as in  $l$ -CdTe (Ref. 10). This is in agreement with Joffe-Regel's empirical rule<sup>15</sup> according to which a liquid behaves like a semiconductor if the short-range order of the crystalline phase is retained.

#### ACKNOWLEDGMENTS

We would like to acknowledge the support for this work by NASA, NSF, and by the Minnesota Supercomputing Institute.

- <sup>1</sup>I. Stich, R. Car, and M. Parrinello, Phys. Rev. B **44**, 4262 (1991).
- <sup>2</sup>P. Silvestrelli, A. Alavi, M. Parrinello, and D. Frenkel, Phys. Rev. Lett. **77**, 3149 (1996).
- <sup>3</sup>G. Kresse and J. Hafner, Phys. Rev. B **49**, 14 251 (1994).
- <sup>4</sup>V. Godlevsky, J. Chelikowsky, and N. Troullier, Phys. Rev. B **52**, 13 281 (1995).
- <sup>5</sup>I. Lee and K. Chang, Phys. Rev. B **50**, 18 083 (1994).
- <sup>6</sup>Q. Zhang, G. Chiarotti, A. Selloni, R. Car, and M. Parrinello, Phys. Rev. B **42**, 5071 (1990).
- <sup>7</sup>C. Molteni, L. Colombo, and L. Miglio, J. Phys.: Condens. Matter **6**, 5255 (1994).
- <sup>8</sup>L. Lewis, A. De Vita, and R. Car, Phys. Rev. B **57**, 1594 (1998).
- <sup>9</sup>R. Kulkarni and D. Stroud, Phys. Rev. B **62**, 4991 (2000).
- <sup>10</sup>V. Godlevsky, M. Jain, J. Derby, and J. Chelikowsky, Phys. Rev. B **60**, 8640 (1999); V. Godlevsky, J. Derby, and J. Chelikowsky, Phys. Rev. Lett. **81**, 4959 (1998).
- <sup>11</sup>J. Gaspard, C. Bergman, C. Bichara, R. Bellissent, P. Chieux, and J. Coffard, J. Non-Cryst. Solids **97/98**, 1283 (1987).
- <sup>12</sup>J. Gaspard, J. Raty, R. Ceolin, and R. Bellissent, J. Non-Cryst. Solids **205-207**, 75 (1996).
- <sup>13</sup>J. Raty, J. Gaspard, R. Ceolin, and R. Bellissent, Physica B **234-236**, 364 (1997).
- <sup>14</sup>M. Ziari, W. Steiner, P. Ranon, M. Klein, and S. Trivedi, Appl. Phys. Lett. **601**, 1052 (1992).
- <sup>15</sup>A. Joffe and A. Regel, *Progress in Semiconductors* (Heywood, London, 1960), Vol. 4, p. 237.
- <sup>16</sup>V. Glazov, S. Chizhevskaya, and N. Glagoleva, *Liquid Semiconductors* (Plenum, New York, 1969).
- <sup>17</sup>P. Rudolph, Prog. Cryst. Growth and Charact. Mater. **29**, 275 (1994).
- <sup>18</sup>P. Kröger, *The Chemistry of Imperfect Crystals* (American Elsevier, New York, 1973), Vol. 1, p. 195.
- <sup>19</sup>V. Godlevsky and J. Chelikowsky, J. Chem. Phys. **109**, 7312 (1998).
- <sup>20</sup>M. Jordan, Metall. Trans. **1**, 239 (1970).
- <sup>21</sup>S. Louie, S. Froyen, and M. Cohen, Phys. Rev. B **26**, 1738 (1982).
- <sup>22</sup>N. Troullier and J. L. Martins, Phys. Rev. B **43**, 1993 (1991).
- <sup>23</sup>D. M. Ceperley and B. J. Alder, Phys. Rev. Lett. **45**, 566 (1980).
- <sup>24</sup>L. Kleinman and D. Bylander, Phys. Rev. Lett. **48**, 1425 (1982).
- <sup>25</sup>*Numerical Data and Functional Relationships in Science and Technology*, edited by O. Madelung, Landolt-Börnstein, New Series, Group III, Vol. 17, Pt. b (Springer-Verlag, Berlin, 1982), pp. 57–60.
- <sup>26</sup>D. Berlincourt, H. Jaffe, and L. R. Shiozawa, Phys. Rev. **129**, 1009 (1963).
- <sup>27</sup>M. Grabow, in *Materials Theory and Modelling*, edited by J. Broughton, P. D. Bristowe, and J. M. Newsam, MRS Symposia Proceedings No. 291 (Materials Research Society, Pittsburgh, 1993), p. 171.
- <sup>28</sup>R. Biswas and D. Hamann, Phys. Rev. B **34**, 895 (1986).
- <sup>29</sup>N. Binggeli, J. L. Martins, and J. R. Chelikowsky, Phys. Rev. Lett. **68**, 2956 (1992).
- <sup>30</sup>O. Sugino and R. Car, Phys. Rev. Lett. **74**, 1823 (1995).
- <sup>31</sup>J. Emsley, *The Elements* (Oxford University Press, Oxford, UK, 1999).
- <sup>32</sup>G. Kresse and J. Hafner, Phys. Rev. B **55**, 7539 (1997).
- <sup>33</sup>M. Yao and H. Endo, J. Non-Cryst. Solids **205-207**, 85 (1996).
- <sup>34</sup>C. Bichara, J. Raty, and J. Gaspard, J. Non-Cryst. Solids **205-207**, 361 (1996).
- <sup>35</sup>R. Kubo, J. Phys. Soc. Jpn. **12**, 570 (1957); D. Greenwood, Proc. Phys. Soc. Jpn. **71**, 585 (1958).
- <sup>36</sup>M. Hybersten and S. Louie, Phys. Rev. B **38**, 4033 (1988).
- <sup>37</sup>A. Oppenheim and R. Schafer, *Discrete-Time Signal Processing* (Prentice-Hall, Englewood Cliffs, NJ, 1989), p. 447.